

(+)- and (-)-Pestaloxazine A, a Pair of Antiviral Enantiomeric Alkaloid Dimers with a Symmetric Spiro[oxazinane-piperazinedione] Skeleton from *Pestalotiopsis* sp.

Yan-Lai Jia,^{†,||,⊥} Mei-Yan Wei,^{†,‡,⊥} Hai-Yan Chen,[§] Fei-Fei Guan,[†] Chang-Yun Wang,^{*,†} and Chang-Lun Shao^{*,†}

[†]Key Laboratory of Marine Drugs, The Ministry of Education of China, School of Medicine and Pharmacy, Ocean University of China, Qingdao, 266003, The People's Republic of China

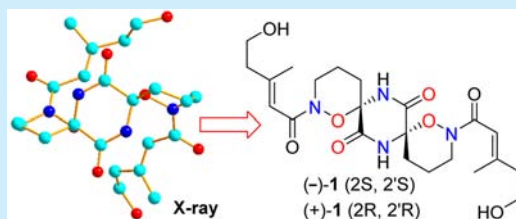
[‡]School of Pharmacy, Guangdong Medical University, Dongguan, 523808, The People's Republic of China

[§]School of Chemistry and Chemical Engineering, Guangxi University, Guangxi Colleges and Universities Key Laboratory of Applied Chemistry Technology and Resource Development, Nanning, 530004, The People's Republic of China

^{||}Shandong Institute for Product Quality Inspection, Jinan, 250102, The People's Republic of China

Supporting Information

ABSTRACT: A pair of new enantiomeric alkaloid dimers, (+)- and (-)-pestaloxazine A (**1**), with an unprecedented symmetric spiro[oxazinane-piperazinedione] skeleton, consisting of 22 carbons and 12 heteroatoms, were isolated from a *Pestalotiopsis* sp. fungus derived from a soft coral. Separation of the enantiomeric alkaloid dimers was achieved by chiral HPLC. Their structures including absolute configurations were elucidated on the basis of a comprehensive analysis of their spectroscopic and X-ray diffraction data and CD calculations. (+)-Pestaloxazine A exhibited potent antiviral activity against EV71 with an IC_{50} value of $14.2 \pm 1.3 \mu\text{M}$, which was stronger than that of the positive control ribavirin ($IC_{50} = 256.1 \pm 15.1 \mu\text{M}$).



Enterovirus 71 (EV71) is a small, single-stranded, positive-sense RNA virus from the *Enterovirus* genus of the *Picornaviridae* family.¹ It causes hand, foot, and mouth disease (HFMD) associated with severe and sometimes fatal neurological complications in young children and infants.² In 2014, the World Health Organization showed that over 2.8 million cases were diagnosed with HFMD in the Western Pacific Region, mainly in China.³ Nevertheless, no vaccine or antiviral drug against EV71 has been approved to date.^{2b,4} As a result, it is imperative to develop new and effective antiviral drugs against EV71 infections.

Marine microorganisms have been recognized as a potential source of structurally novel and biologically potent metabolites.⁵ More significantly, material supply of bioactive compounds produced by microorganisms including those from marine sources may not be limited because of their culturability. To search for a resource for bioactive compounds, we have focused our efforts on fungi derived from marine invertebrate, especially those that are derived from corals in the South China Sea.⁶ Further chemical investigation of the fermentation broth of a *Pestalotiopsis* sp. (ZJ-2009-7-6) fungus derived from a soft coral⁷ resulted in the isolation and identification of an alkaloid dimer with an unprecedented symmetric spiro[oxazinane-piperazinedione] skeleton, named pestaloxazine A (**1**) (Figure 1),⁸ which exhibited potent and selective antiviral activity against EV71. Herein, we report the isolation, structure elucidation, chiral HPLC separation, CD

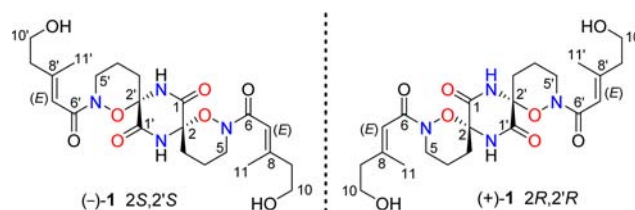


Figure 1. Structures of (-)-**1** (2S, 2'S) and (+)-**1** (2R, 2'R).

calculations, plausible biogenetic pathway, and antiviral activity of this new alkaloid dimer.

The fungal strain *Pestalotiopsis* sp. (ZJ-2009-7-6) was cultivated on solid rice medium in 30 Erlenmeyer flasks at 28 °C without shaking for 13 weeks. Then the culture was extracted two times with EtOAc and one time with $\text{CH}_2\text{Cl}_2/\text{MeOH}$ (v/v, 2:1). The organic extracts were combined and concentrated under vacuum to afford a dry crude extract. Purification of the extract by silica gel column chromatography (CC), Sephadex LH-20 CC, and HPLC yielded **1** (7.2 mg).

(±)-Pestaloxazine A (**1**) was obtained as colorless crystals. Their pseudomolecular ion peaks were observed at m/z 481.3 $[\text{M} + \text{H}]^+$, 503.3 $[\text{M} + \text{Na}]^+$, and 983.6 $[2\text{M} + \text{Na}]^+$ in the ESI-MS spectrum. Its molecular formula of $\text{C}_{22}\text{H}_{32}\text{N}_4\text{O}_8$ (9 degrees

Received: July 13, 2015

Published: August 20, 2015

of unsaturation) was based on the HR-ESI-MS peak at m/z 481.22944 $[M + H]^+$. The IR absorption bands at 1702 and 1713 cm^{-1} suggested the presence of amide groups, which were supported by the presence of two carbonyl signals at δ_C 168.3 and δ_C 166.2 in the ^{13}C NMR spectrum. The UV absorption at 216 nm and HMBC spectrum indicated that the methyl group (δ_H 2.09, δ_C 19.3) was attached to a trisubstituted olefin. With the exception of exchangeable protons, analysis of the NMR data (Table 1) showed signals for 11 carbons and 14 protons,

Table 1. ^1H NMR (500 MHz) and ^{13}C NMR (125 MHz) Data of Pestaloxazine A in CD_3OD (δ in ppm)

position	δ_C	δ_H , mult (J in Hz)
1	166.2, C	
2	87.3, C	
3	30.9, CH_2	2.58, 1.79 (1H each, m)
4	19.0, CH_2	2.16, 1.93 (1H each, m)
5	42.6, CH_2	3.89, 3.78 (1H each, m)
6	168.3	
7	117.6, CH	6.42 (1H, s)
8	155.5	
9	44.9, CH_2	2.31 (2H, t, $J = 6.9$)
10	61.3, CH_2	3.64 (2H, t, $J = 6.9$)
11	19.3, CH_3	2.09 (3H, s)
10-OH ^a		4.45 (s)
NH ^a		9.79 (s)

^aRecorded in $\text{DMSO}-d_6$.

only accounting for half of the numbers expected from the molecular formula, which indicated that the compound **1** should have a symmetrical structure.

The ^1H NMR spectrum revealed these signals for one olefinic proton (δ_H 6.42, 1H, s), one methyl (δ_H 2.09, 3H, s), and ten methylene protons (δ_H 2.31, 3.64, each 2H, t, $J = 6.9$ Hz; and δ_H 1.79, 1.93, 2.16, 2.58, 3.78, 3.89, each 1H, m). Furthermore, two exchangeable protons at δ_H 9.79 and 4.45 were observed in $\text{DMSO}-d_6$. The 11 carbon signals showed in the ^{13}C NMR and DEPT spectra of **1** could be classified as five methylenes including one nitrogenated and one oxygenated methylene, one olefinic methine (δ_C 117.6), and four quaternary carbons (one aliphatic, one olefinic, and two amide carbonyls), and one methyl group (δ_C 19.3). The nine degrees of unsaturation inherent in the molecular formula of **1**, coupled with the NMR data showing the presence of two carbonyl groups and two olefinic carbons (2-fold of three degrees of unsaturation as the dimer), indicated that the dimer should possess three rings.

By analysis of 1D and 2D NMR spectra (COSY, NOESY, HSQC, and HMBC), two partial structures (I and II, Figure 2) were established, again accounting for only half of the total number of atoms in the molecular formula. As noted above, HMBC correlations of the lone olefinic proton H-7 to C-9/C-11 and H-11 to C-6/C-7/C-8/C-9 allowed the formation of a trisubstituted-unsaturated amide moiety. Moreover, HMBC correlations from H-9 to C-7/C-8/C-10, from H-10 to C-8/C-9, and from 10-OH to C-9 allowed extension of substructure I to include the COSY-derived sequence C-9–C-10. Similarly, substructure II (C-1/C-2/C-3/C-4/C-5, was identified on the basis of COSY correlations between H-3/H-4/H-5, together with HMBC correlations of H-3 to C-1/C-2/C-5, H-4 to C-5, and NH to C-1 and C-2. The methylene group with a relatively downfield proton chemical shift at δ_H 3.78 and 3.89 (H_2 -5) and

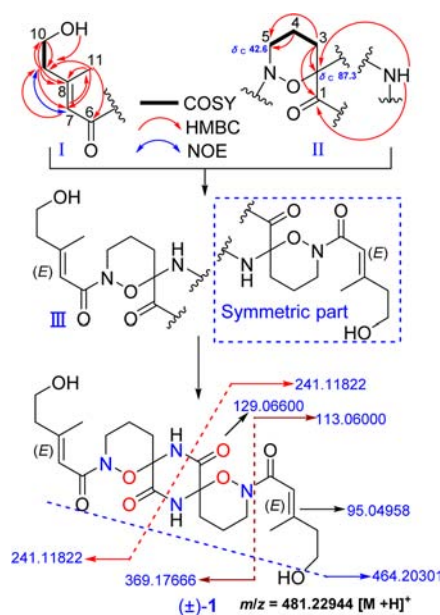


Figure 2. Partial structures and key ^1H – ^1H COSY, HMBC, and NOESY correlations together with the Q-Exactive-HR-ESI-MS² fragment ions used to establish the gross structure of **1**.

relatively upfield carbon chemical shift at δ_C 42.6 (C-5) indicated that it was an *N*-methylene group rather than an *O*-methylene group. The quaternary carbon of C-2 was tentatively assigned to a hemiaminal group based on the chemical shift of C-2 at δ_C 87.3 together with the available heteroatoms in the molecular formula. The N–O bond was formed to construct an oxazinane ring on the basis of the degree of unsaturation. The connection of the amide bond between the partial structures I and II was hindered and could be postulated on the basis of the remaining unassigned amide carbonyl at δ_C 168.3 and one bond of the nitrogen atom (5-N), although no HMBC correlation between H-5 and C-6 was observed (III, Figure 2). The geometry of the C-7–C-8 double bond was defined by an NOE experiment (Supporting Information). NOE correlations between H-7 (δ_H 6.42, 1H, s) and H₂-9 (δ_H 2.31, t, $J = 6.9$ Hz) were observed, indicating an olefin of *E*-configuration. Moreover, a correlation from the exchangeable proton at δ 8.96 (NH) to a carbonyl carbon at δ_C 166.2 (C-1) and a quaternary carbon at δ_C 87.3 (C-2) indicated attachment via an amide bond. On the basis of the analysis above, the gross structure of **1** was deduced to possess a piperazinedione skeleton as shown in Figure 2. It should be mentioned that NMR data ultimately proved to be insufficient to solve the structure of pestaloxazine A (**1**). Besides, additional evidence that further confirmed the gross structure of **1** came from the Q-Exactive-HR-ESI-MS² experiment that illustrated prominent fragment ions in support of the structure (Figure 2).

To elucidate the structure unambiguously, we undertook a single X-ray diffraction study. Ultimately, by slow crystallization in MeOH, single crystals of **1** suitable for X-ray diffraction analysis were obtained allowing the planar structure and relative configuration of **1** to be confirmed (Figure 3).⁹ Further analysis of the X-ray data revealed that **1** possessed a centrosymmetric space group $P\bar{1}$, indicating its racemic nature. In order to clarify the racemic mixture of **1**, HPLC analysis of **1** on a chiral column (Kromasil 5-TBB) was carried out. Two distinct chromatographic peaks with a ratio of 1:1 were found and isolated. The CD spectra of (+)-**1** and (–)-**1** displayed similar

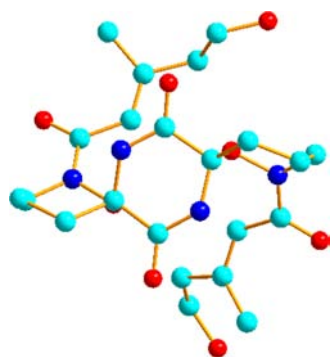


Figure 3. Single-crystal X-ray structure of (±)-1.

signal intensity but opposite Cotton effects, confirming their enantiomeric relationship (Figure 4a).

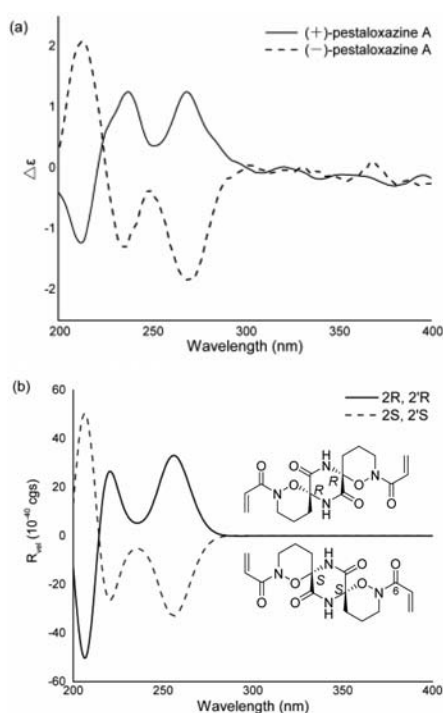
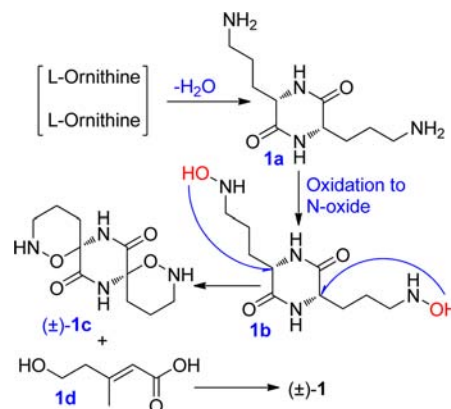


Figure 4. (a) Experimental CD spectra for **1** and (b) calculated ECD spectra for simplified model compound of **1**, respectively.

Based on the relative configurations, the absolute configurations of the two enantiomers of **1** were confirmed by comparing the theoretical calculation ECD with the experimental CD (Supporting Information). Since **1** has a long side chain, the conformations of the compound are too large. Then, **1** was simplified to two model compounds (Figure 4b). The model compounds' ECDs were performed by the TD-DFT [PCM/MeOH/PBE0/Aug-cc-pVDZ//B3LYP/6-311++G(d,p)]. The CD of (+)-**1** is similar to the ECD of the model compound (2*R*, 2'*R*), and the CD of (-)-**1** is similar to the ECD of (2*S*, 2'*S*). Therefore, the stereostructures of (+)-**1** and (-)-**1** were established as 2*R*, 2'*R* and 2*S*, 2'*S* (Figure 4).

A proposed biosynthetic pathway to **1** starting from two molecules of L-ornithine is shown in Scheme 1. Double dehydration leads to the piperazinedione intermediate (**1a**). Then, the oxidation forms the *N*-oxide (**1b**), followed by intermolecular nucleophilic attack at the same face to give the

Scheme 1. Plausible Biosynthetic Pathway to **1**



key intermediate (±)-**1c** which comprises a pair of racemates. Finally, (±)-**1** could be formed by condensation between **1c** and **1d**. Theoretically, a pair of epimers of (±)-**1**, the epimer (2*R*, 2*S'* or 2*S*, 2'*R'*) of (±)-**1**, a mesomer, was not observed indicating that the production of pestaloxazine A in the fungus was regulated by the enzymes with selective catalytic functions.

According to the anti-EV71 (enterovirus 71) assay on the Vero cell line *in vitro* using the CPE inhibition assay,¹⁰ (±)-**1**, (+)-**1**, and (-)-**1** showed different antiviral activity with IC₅₀ values of 16.0 ± 0.8, 14.2 ± 1.3, and 69.1 ± 3.1 μM, respectively (Table 2). Especially, promising antiviral activity

Table 2. Antiviral Activity of (+)-**1**, (-)-**1**, and (±)-**1** against EV71^a

compound	EV71		
	TC ₅₀ (μM)	IC ₅₀ (μM)	SI
(+)- 1	130.2 ± 10.1	14.2 ± 1.3	9.2
(-)- 1	143.7 ± 8.9	69.1 ± 3.1	2.1
(±)- 1	126.6 ± 6.6	16.1 ± 0.8	7.9
ribavirin	>4098	256.1 ± 15.1	>16

^aCytotoxicity (TC₅₀) and antiviral activity (IC₅₀) were determined by the CPE inhibition assay on Vero cells. Selectivity index (SI) is the ratio of TC₅₀ to IC₅₀. Data were expressed as means ± SD of three independent experiments.

was exhibited by (+)-**1**, which was approximately 18-fold more potent than ribavirin (IC₅₀ = 256.1 ± 15.1 μM). Moreover, the selectivity indices (SI) of anti-EV71 activity of (±)-**1**, (+)-**1**, and (-)-**1** were 7.9, 9.2, and 2.1, respectively. These results indicated that the stereochemistry of the spiro center might contribute to the antiviral activity and selectivity indices. These compounds were also tested against three other viruses, namely the respiratory syncytial virus (RSV), Coxsackie B3 (Cox-B 3), and H1N1, but they did not show any activity.

Pestaloxazine A belongs to the mixed polyketide-cyclo-dipeptide class of natural products (often referred to as a PKS-NRPS hybrid). Its structure is unique for several reasons, including its unprecedented symmetric spiro[oxazinane-piperazinedione] skeleton and two unique hemiaminal and oxazinane groups. It consists of 22 carbons and 12 heteroatoms with 10 of the 22 carbons either oxygenated or nitrogenated, and this also contributes to its highly unusual structure. The pestaloxazine is also of interest because it is the first of this kind.

The unique carbon skeletons of the pestaloxazines from a fungus of the genus *Pestalotiopsis* sp. clearly indicate the tremendous potential of fungi derived from soft corals as a source of novel secondary metabolites.

In summary, we have described the isolation and structure elucidation of a pair of novel enantiomeric alkaloid dimers from a *Pestalotiopsis* sp. fungus derived from a soft coral. (+)-Pestaloxazine A (**1**) exhibited potent and selective antiviral activity and represents a promising new class of antiviral agent. Further studies on evaluating its *in vivo* activity, ¹³C-labeling feeding experiments, and structure–activity relationships, are in progress.

■ ASSOCIATED CONTENT

■ Supporting Information

The Supporting Information is available free of charge on the ACS Publications website at DOI: 10.1021/acs.orglett.5b01995.

¹H, ¹³C NMR, DEPT, HSQC, HMBC, ¹H–¹H COSY, NOESY, ESI-MS, HR-ESI-MS², HR-ESI-MS spectra, and Chiral HPLC spectrum of the new compound **1**, CD and calculated ECD data for compounds (+)-**1** and (–)-**1**, together with experimental details (PDF) X-ray crystallographic data for **1** (CIF)

■ AUTHOR INFORMATION

Corresponding Authors

*E-mail: changyun@ouc.edu.cn.

*E-mail: shaochanglun@163.com.

Author Contributions

¹Y.-L.J. and M.-Y.W. contributed equally.

Notes

The authors declare no competing financial interest.

■ ACKNOWLEDGMENTS

We thank Prof. Yu-Cheng Gu and Dr. John Clough (Syngenta) for their proofreading of the manuscript and Dr. Xin Liu (Beijing CIQ) for the HR-ESI-MS spectrum. This work was supported by the Program of National Natural Science Foundation of China (Nos. 41322037, 41176121, 21102022, and 41130858) and the Program of National Natural Science Foundation of Shandong Province of China (No. JQ201510). We also thank the High-Performance Computing Platform of Guangxi University for generous support of our computational chemistry research.

■ DEDICATION

Dedicated to Professor Yongcheng Lin, Sun Yat-sen University, on the occasion of his 70th birthday.

■ REFERENCES

- (1) Oberste, M. S.; Maher, K.; Kilpatrick, D. R.; Pallansch, M. A. *J. Virol.* **1999**, *73*, 1941–1948.
- (2) (a) Ooi, M. H.; Wong, S. C.; Lewthwaite, P.; Cardosa, M. J.; Solomon, T. *Lancet Neurol.* **2010**, *9*, 1097–1105. (b) McMinn, P. C. *FEMS Microbiol. Rev.* **2002**, *26*, 91–107. (c) Qiu, J. *Lancet Neurol.* **2008**, *7*, 868–869.
- (3) WHO. Wpro hand, foot and mouth disease situation update, 27 January 2015. Available online: http://www.wpro.who.int/emerging_diseases/hfmdbiweekly_13jan2015.pdf?ua=1 (accessed Jul. 1, 2015).

- (4) (a) Shang, L.; Xu, M.; Yin, Z. *Antiviral Res.* **2013**, *97*, 183–194. (b) Wu, K. X.; Ng, M. M. M.; Chu, J. J. H. *Drug Discovery Today* **2010**, *15*, 1041–1051.

- (5) (a) Blunt, J. W.; Copp, B. R.; Keyzers, R. A.; Munro, M. H. G.; Prinsep, M. R. *Nat. Prod. Rep.* **2015**, *32*, 116–211. (b) Newman, D. J.; Cragg, G. M. *J. Nat. Prod.* **2012**, *75*, 311–335. (c) Gerwick, W. H.; Moore, B. S. *Chem. Biol.* **2012**, *19*, 85–98.

- (6) (a) Wei, M. Y.; Wang, C. Y.; Liu, Q. A.; Shao, C. L.; She, Z. G.; Lin, Y. C. *Mar. Drugs* **2010**, *8*, 941–949. (b) Shao, C. L.; Wu, H. X.; Wang, C. Y.; Liu, Q. A.; Xu, Y.; Wei, M. Y.; Qian, P. Y.; Gu, Y. C.; Zheng, C. J.; She, Z. G.; Lin, Y. C. *J. Nat. Prod.* **2011**, *74*, 629–633. (c) Shao, C. L.; Wang, C. Y.; Wei, M. Y.; Gu, Y. C.; She, Z. G.; Qian, P. Y.; Lin, Y. C. *Bioorg. Med. Chem. Lett.* **2011**, *21*, 690–693. (d) Yang, K. L.; Wei, M. Y.; Shao, C. L.; Fu, X. M.; Guo, Z. Y.; Xu, R. F.; Zheng, C. J.; She, Z. G.; Lin, Y. C.; Wang, C. Y. *J. Nat. Prod.* **2012**, *75*, 935–941. (e) Qin, X. Y.; Yang, K. L.; Li, J.; Wang, C. Y.; Shao, C. L. *Mar. Biotechnol.* **2015**, *17*, 99–109.

- (7) Wei, M. Y.; Li, D.; Shao, C. L.; Deng, D. S.; Wang, C. Y. *Mar. Drugs* **2013**, *11*, 1050–1060.

- (8) Pestaloxazine A (**1**): colorless crystals; [α]_D²⁰ 0 (c 0.10, CH₃OH); UV (MeOH) λ_{\max} (log ϵ) 216 (3.98) nm; IR (KBr) ν_{\max} 3750, 3419, 1713, 1702, 1599, 1455 cm⁻¹; ESI-MS *m/z* 481 [M + H]⁺, 503 [M + Na]⁺, 983 [2M + Na]⁺; HR-ESI-MS *m/z* 481.22944 [M + H]⁺ (calcd for C₂₂H₃₃N₄O₈, 481.22984). For ¹H and ¹³C NMR data, see Table 1. (+)-**1**: [α]_D²⁰ +1.09 (c 0.10, CH₃OH); CD (MeOH) λ_{\max} ($\Delta\epsilon$) 212 (–1.34), 235 (+1.31), 268 (+1.32) nm. (–)-**1**: [α]_D²⁰ –3.22 (c 0.14, CH₃OH); CD (MeOH) λ_{\max} ($\Delta\epsilon$) 212 (+2.10), 235 (–1.31), 269 (–1.84) nm.

- (9) Crystal data for **1**: C₂₂H₃₄N₄O₉, *M*_r = 498.53, Triclinic, space group $P\bar{1}$ with *a* = 9.7492(19) Å, *b* = 10.793(2) Å, *c* = 12.316(3) Å, α = 106.75(3)°, β = 97.22(3)°, γ = 95.45(3)°, *V* = 1219.4(4) Å³, *Z* = 2, *D*_x = 1.358 mg/m³, μ (MoK α) = 0.71073 mm⁻¹, and *F*(000) = 532. Crystal dimensions: 0.23 × 0.20 × 0.19 mm³. Independent reflections: 4523. The final *R*₁ values were 0.0756, *wR*₂ = 0.1010 (*I* > 2 σ (*I*)). Crystallographic data have been deposited in the Cambridge Crystallographic Data Centre (deposition number CCDC 1400359).

- (10) Grassauer, A.; Weinmuellner, R.; Meier, C.; Pretsch, A.; Prieschl-Grassauer, E.; Unger, H. *Virol. J.* **2008**, *5*, 107.